Application of Reactive Bonding Methods on LTCC Substrates

Erik Wiss
Chair of Microintegration and Reliability
Saarland University
Saarbruecken, Germany
erik.wiss@uni-saarland.de

Alexander Schulz
Electronics Technology Group
TU Ilmenau
Ilmenau, Germany
alexander.schulz@tu-ilmenau.de

Adam Yuile
Chair of Microintegration and Reliability
Saarland University
Saarbruecken, Germany
adam.yuile@uni-saarland.de

Jens Mæller
Electronics Technology Group
TU Ilmenau
Ilmenau, Germany
jens.mueller@tu-ilmenau.de

Steffen Wiese
Chair of Microintegration and Reliability
Saarland University
Saarbruecken, Germany
s.wiese@mx.uni-saarland.de

Abstract ¯ This paper discusses the application of reactive bonding for the area of Low Temperature Cofired Ceramics (LTCC) assemblies. The goal is to reduce the thermal-mechanical stresses during soldering by transferring heat only locally to the solder joints without heating the entire component. Such a reactive multilayer system (RMS) consists of alternating nanolayers (10 - 300 nm) of at least two metal components which produce an exothermal reaction after ignition. Although the deposition of an RMS is established on silicon substrates for the use in micro-electromechanical systems (MEMS), it is very challenging to create them on LTCC substrates. One of the main obstacles is to overcome all issues connected with the significant roughness, because it is not an optimum territory to deposit nanolayers. In this paper, different methods like chemical mechanical polishing (CMP) and laser ablation, to modify the surface morphology, are presented. A direct relation between the morphology and the exothermal reaction can be observed. In addition, 3-D Computational Fluid Dynamics (CFD) simulations were conducted to analyze the process in more detail. These simulations make use of a shoebox model with different layers and an adjustable user-defined function for the heat release of the RMS to adapt the reaction front velocity and the combustion temperature to the experimental values.

Keywords ¯ LTCC, RMS, reactive multilayer systems, Al-Ni, joining.

I. Introduction

The chemical reaction of nitrogen monoxide (NO) with ozone leads not only to the formation of nitrogen dioxide and oxygen, but also to the emission of radiation in the wavelength range between 600 to 2600 nm with a maximum in the infrared area at 1200 nm [1]. Measuring this radiation can be used to determine low concentrations of NO in gas flows. Therefore, a measurement device was developed and presented in [2]-[4] using LTCC (Low Temperature Cofired Ceramics) technology (see Fig. 1). It consists of three different modules: first, there is an ozone generator with a high voltage source, that is applied to a gas flow using embedded electrodes. Then, the ozone is transported via microfluidic channels to a chemiluminescence detection reaction chamber where it is mixed with the gas that contains an unknown amount of NO. An infrared transparent window is bonded onto the LTCC substrate, and a photo diode that measures the emitted radiation is placed on it. The last module is an exhaust gas treatment to decompose the ozone into nonhazardous oxide. Therefore, a heating structure was embedded in the LTCC substrate and a platinum paste, that can be applied to the substrate, was used as a catalysator.

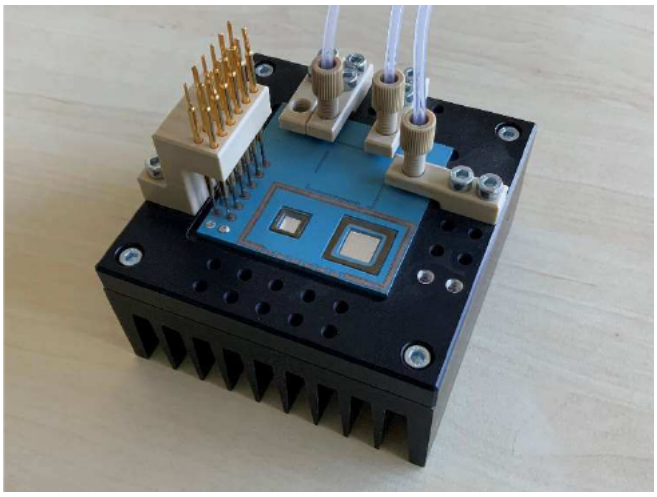

Fig. 1. Measurement device for low concentrations of nitrogen monoxide in gas flows, realized using LTCC technology.

The LTCC technology is an excellent candidate for such devices because it enables the possibility of three-dimensional structuring [5]-[7] and shows very good hermetic sealing properties [8], [9]. Additionally, it provides not only excellent robustness under harsh environmental and mechanical conditions [10], [11], but also chemical resistance [9]-[13]. Due to this properties, LTCC technology can even be used in automotive and aerospace. It is also possible to add passive elements using conventional surface mounting technology like reflow soldering. Therefore, both the component and the substrate need to be heated up to a temperature above the melting point of the used solder, which can be critical for heat sensitive components. Adding heat locally to the solder joints can be an option to avoid damages during this process e.g., through using a reactive multilayer system (RMS). While the use of an RMS is well established on silicon substrates [14], it is very challenging to deposit such a system on LTCC substrates due to their high roughness in the range of 0.4 to 1 ı m [15]-[17].

An RMS consists of at least two different materials that are applied on a substrate in an alternating way e.g., through

magnetron sputtering [10]. The thickness of every single layer is in the range of 10 to 300 nm [19] and the total stack thickness varies in the range of 0.1 to 300 ı m [20]. After the system is ignited (e.g., by providing sufficient heat, by using an electrical spark or by using a laser pulse) the materials begin to intermix on atomic level building a new intermetallic phase. This leads to a self-propagating reaction [21] that is profoundly exothermal [22]. The released heat of this process can be used for joining processes by melting an additional solder layer, among other things. The propagation speed will depend on the materials used, the bilayer thicknesses, the ratio of the materials, the total stack thickness and the amount of heat released. However, the mechanical pre-processing of the substrates also has an influence on the speed of the reaction, what should be discussed here.

II. Sample preparation

A. Reference sample and laser ablation

As described in [23] the samples were prepared in different ways. For the reference samples, and the samples that were modified by laser ablation, a standard LTCC technology was processed using 6-layer DuPont 951 P2 resulting in a thickness of 817 nm ě 2.5 nm. Without further processing a roughness of 390 nm ě 16.6 nm was reached for the reference samples.

To achieve other roughnesses the surface of the LTCC substrate was laser ablated in a grid-like way using a 355 nm picosecond UV laser system. Different cutting distances between 5 and 30 ı m and a laser power between 0.5 W and 1 W were used, which resulted in a roughness between 572 nm ě 14.4 nm and 874 nm ě 20.5 nm. Finally, the samples were cut into pieces of 15 mm x 7 mm. After that a 20 nm thick layer of titanium was sputtered onto the samples as an adhesion layer, followed by the subsequentially deposition of the RMS. With a total thickness of 10 ı m, 100 bilayers were chosen with a thickness of 60 nm for the aluminum and 40 nm for the nickel. After processing the samples, they were ignited by an electrical spark using two electrodes and a power supply limited to 25 V and 4 A.

B. Chemical/mechanical lapping and polishing (CMP)

The other possibility for the sample preparation persists in using a CMP machine to achieve lower roughness. An 8-layer DuPont 951 P2 was processed in a standard LTCC technology resulting in a thickness of 1080 ı m. The substrates were lapped down chemically/mechanical on both sides to achieve a plane surface with a thickness of 810 ı m ě 5,5 ı m. Further polishing led to a roughness in the range between 105 nm ě 19.5 nm and 258 nm ě 16.5 nm. As before the samples were cut into smaller pieces and both the adhesion layer and the RMS were deposited.

C. Laser ablation with additional metallization

Some samples obtained an additional AgPd metallization between the LTCC substrate and the RMS [24]. Therefore, a standard LTCC technology was processed using 4-layer DuPont 951 PX resulting in a thickness of 839 ı m ě 2.6 ı m. The surface morphology was modified using the laser system in the same way as before. The reference sample (without further processing) reached a roughness of 525 nm ě 30 nm, whereas the other ones reached a roughness of 537 nm ě 12 nm (LS 3) and 773 nm ě 29 nm (LS 5). Finally, the samples were cut into pieces of 15 mm x 7 mm and the RMS was deposited.

D. Roughness characterization

The roughness of the surface was characterized by using a laser scanning microscope [23], [24]. An area of 250 ı m x 250 ı m was chosen for the measurements. The lowest roughness of about 100 nm was found for the CMP samples without metallization whereas the laser ablated samples show the highest roughness with a maximum of about 870 nm. Without processing the roughness is about 400 nm (see Fig. 2). For the samples with metallization, a roughness of 525 nm (reference) respectively 537 nm and 773 nm were reached (laser ablated samples).

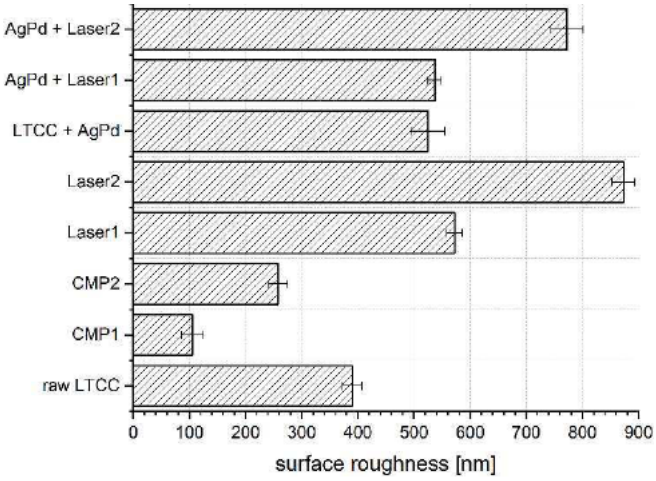

Fig. 2. Resulting surface roughness for some samples with different preparation methods, measured by LSM [23], [24].

III. CFD model

A. CFD model description

To achieve more information about the reactive joining process a suitable CFD model was already developed and presented in [25]-[27] (see Fig. 3). It consists of the aluminum-nickel bilayer (blue), the LTCC substrate (green) and the isolation layer (green) between, some simulations also contain a solder layer. The base of the model has a primary surface of 4 mm x 4 mm with a surrounding air environment of the dimensions 10 mm x 10 mm x 5 mm to avoid interactions between the region of interest and the boundary conditions. Due to stability and convergence reasons no titanium layer was considered in the simulation model.

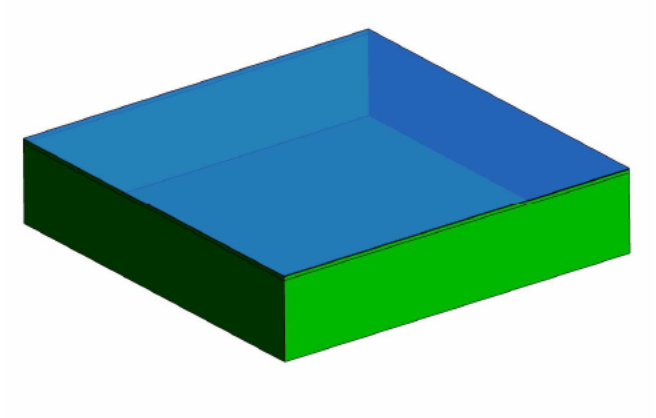

Fig. 3. The CFD simulation model mainly consists of the reactive multilayer system (blue) and the LTCC substrate with an isolation layer (green) [25].

The material properties and the dimensions of the individual layers are shown in Table I. The properties of the LTCC substrate and the isolation layer were assumed to be identical (GreenTape™ DuPont DP951), which is why the effective thickness of the LTCC substrate is 860 ı m. The properties of the RMS match with an unreacted multilayer [28], and the properties for the solder and the silicon chip were taken from the ANSYS Fluent material databases.

Table I. Dimensions and properties of the layers used in the CFD simulation model [26], [28].

layer	thickness [ı m]	[illegible] [kg/m³]	[illegible] [W/mðK]	[illegible] [J/kgðK]
LTCC	825	3100	3.3	600
Isolation	35	3100	3.3	600
RMS	30	5500	152	830
Solder	200	7000	63.2	230
Chip	400	2500	100	710

A 3x3 matrix of temperature probes was used to measure the temperatures during the movement of the reaction front. The probes in the same vertical position (e.g., P1, P2, P3) give information about the reaction velocity (through the time delay in the recorded values), and the probes in the same horizontal direction (e.g., P1, P4, P7) can be used to determine the peak temperature. For additional information the temperatures were also measured in the middle of the RMS, at the interface between the RMS and the solder, and at distances of 10 and 20 ı m in the solder starting from the interface.

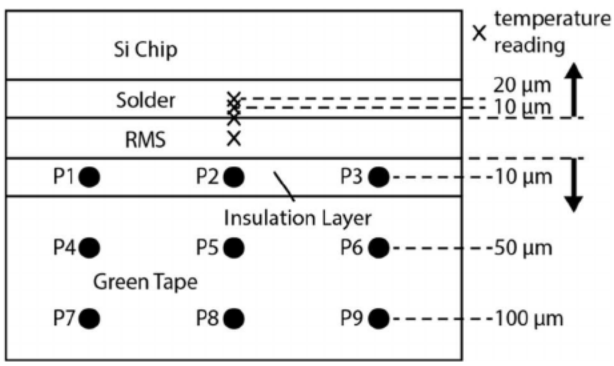

Fig. 4. Locations of the platinum temperature probes (P1 to P9) and the measurement points in the solder and the RMS.

All the structures were meshed in ANSYS Workbench 2023R1 with a length of 100 ı m for the mesh edges in x- and y-direction, and with a length of 10 ı m in the z-direction leading to a total number of 5,001,000 cells. The time-step size was fixed to 10^{-6} s for 10,000 time-steps which results in a simulation time of 10 ms. For a more detailed view see [25], [26]. To simulate the propagation of the reaction front, a probability density function in the form of (1) was used.

[illegible] (1)

The four parameters A, B, C and D are used to control the heat release function, where A and B approximately correspond to the amplitude and width, C is an offset for the alignment with the leading edge of the reactive multilayer system and D corresponds to the velocity.

IV. Results

A. Experimental analysis

As described in [23], all the samples showed a good adhesion behavior before ignition (see Fig. 5). After ignition, a peel-off effect could be observed at both the unmachined reference sample and the CMP prepared samples with low roughness (105 ǔ 390 nm). In contrast the samples that were laser ablated with a roughness between 572 nm and 874 nm still show a good adhesion even after ignition, but SEM images show the occurrence of micro cracks within the RMS. Both the micro cracks and the peel-off effect are mainly caused by the different coefficients of thermal expansion of the materials. As an additional factor, there is a shrinkage in volume of approximately 12 % in the RMS due to lattice-spacing reduction [29] which may also affect the adhesion.

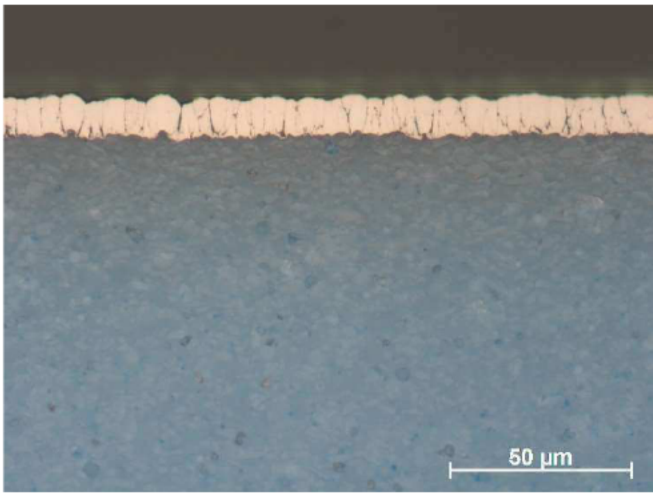

Fig. 5. Reflected light microscopy image reveals a good adhesion of the reactive multilayer on the LTCC substrate (blue) before ignition.

To determine the peak temperatures and the reaction speed, high velocity pyrometer measurements and high-speed camera measurements were done simultaneously [23], [24]. The pyrometer measurements show that the unmachined LTCC substrate reaches the highest peak temperature (1092 éC), followed by the samples that were prepared by CMP with nearly the same temperature (1067 and 1062 éC). The samples that were prepared by laser ablation reach the lowest temperatures (811 and 803 éC). It is remarkable that there is nearly no difference within the laser ablated samples although they differ in their roughness (572 nm to 873 nm). It can be assumed that the higher temperatures occur due to the peel-off of the RMS: the heat cannot be dissipated through the air as fast as if the RMS was still in contact with the substrate.

In case of the laser ablated samples with AgPd metallization, the lift-off effect was not as pronounced as in the other samples without the metallization. There is a punctual adhesion of the reactive multilayer, whereas some areas are separated from the metallization (see Fig. 6). The reference sample reaches a peak temperature of 854 éC whereas the laser ablated samples reach 847 and 739 éC. This temperature drop (compared to the first samples) may be caused by the additional metallization layer that absorbs some of the released heat.

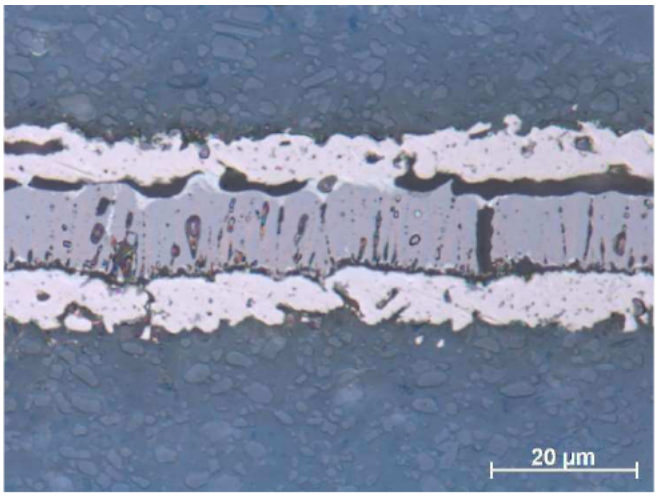

Fig. 6. Reflected light microscopy image of a reactive multilayer system between two LTCC substrates (blue) with AgPd metallization (bright areas) after ignition. There is only punctual adhesion of the RMS, whereas most areas of the RMS separated from the metallization.

The high-speed measurements show a velocity of around 5 m/s for the reaction front of both the reference sample and the CMP prepared samples. In contrast, the laser ablated samples show a reduction in velocity down to 3.7 m/s (roughness 572 nm) and 2.9 m/s (roughness 873 nm). The same effect can be observed on the samples with AgPd metallization: the velocity reduces from 3.7 m/s (roughness 525 nm) to 2.8 m/s (roughness 537 nm) and 2.2 m/s (roughness 773 nm). The measured values are clearly represented in Table II.

Table II. Overview of the reached peak temperatures and reaction front velocities depending on different substrate preparation methods and resulting surface roughness [23], [24].

	substrate preparation	surface roughness [nm]	peak temp. [éC]	reaction front velocity [m/s]
LTCC without metallization	CMP 1	105	1067	5.1
	CMP 2	257	1062	4.7
	Ref.	390	1092	5.1
	LS 1	572	811	3.7
	LS 2	873	803	2.9
LTCC with metallization	AgPd + Ref.	525	854	3.7
	AgPd + LS 3	537	847	2.8
	AgPd + LS 5	773	739	2.2

B. CFD comparisons

Simulations were performed for a model with solder (Fig. 7) and for a model without solder (Fig. 8). A velocity for the reaction front of 1 m/s and a time-step size of 10^{-6} s was chosen for the temperature recordings.

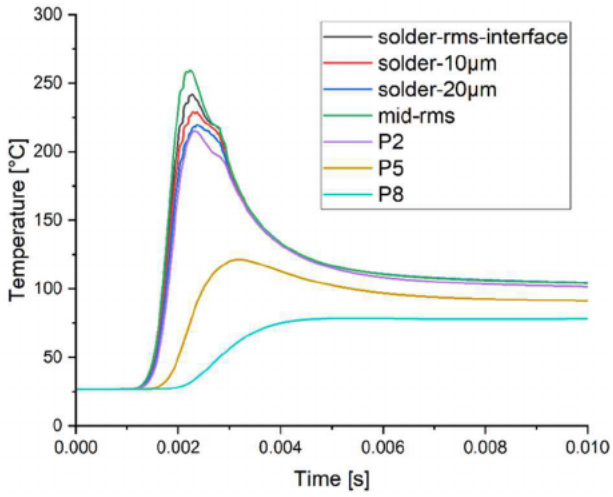

Fig. 7. Temperature contour plot of the interface between the solder and RMS, within the solder and the RMS, and at the temperature probes P2, P5 and P8 for a velocity of 1 m/s.

As depicted in Fig. 7 the maximum temperature of about 260 éC was reached within the RMS which is only slightly above the required temperature of 240 éC [26]. At the interface between the RMS and the solder it reaches around 240 éC and the lowest value with around 220 éC is reached at a distance of 20 ı m within the solder.

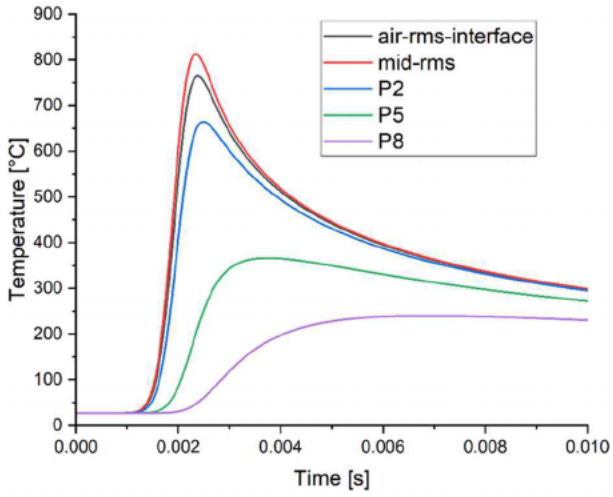

Fig. 8. Temperature contour plot for the model without solder of the interface between the air and RMS, within the RMS and at the temperature probes P2, P5 and P8 for a velocity of 1 m/s.

Fig. 8 shows the temperature plot for the model without a solder layer. The reached temperature within the RMS is raised by more than 200 % up to 820 éC while the temperature at the interface between the surrounding air and the RMS is above 750 éC. By comparison to the previous model, it can be assumed that the melting and solidification of the solder is responsible for this significant drop of the RMS peak temperature, so the amount of solder deposited on the RMS should be a good parameter to control the peak temperature during reactive bonding. A similar relation was already considered by Wang [30].

V. Conclusions

This paper discusses the application of reactive bonding methods on LTCC substrates. Therefore, a reactive multilayer system (RMS) consisting of alternating nanolayers of

aluminum and nickel with a total thickness of 100 ı m was deposited after two different surface modifications were applied. Then, the samples were electrically ignited which was recorded by a high velocity pyrometer and a high-speed camera for temperature and velocity measurements. The first preparation method is chemical mechanical polishing (CMP) of a LTCC substrate, without metallization, which lowers the surface roughness down to around 100 nm. Compared to the reference sample (roughness 390 nm), the CMP does not seem to influence the peak temperature or the reaction front velocity. In addition, there is a peel-off of the RMS structure. The second method uses a picosecond laser to modify the LTCC substrate morphology, whereby the roughness can be increased up to 873 nm. This leads to a decrease in the peak temperature by nearly 300 éC and a decrease in the reaction front velocity by around 27 - 43 %. In case of the laser ablated surfaces no peel-off effects could be observed but some micro cracks in the RMS could be found. Both the peel-off effects and the micro cracks occur due to different coefficients of thermal expansion and the volume shrinkage during the exothermal reaction. An additional reason for the problems in adhesion is the lower thermal conductance of the LTCC substrate compared to silicon substrates.

Laser ablation was also done for samples with an additional AgPd metallization between the LTCC substrate and the deposited RMS. After ignition, less peel-off effects could be observed. The drop in the RMS peak temperature is not as high as in the other version, but the velocity of reaction front was slowed down by around 24 - 41 %. The experimental data show that the adhesion still has to be improved.

CFD simulations were conducted to analyze the process in more detail. A shoebox model with the different layers (LTCC, RMS and solder) was presented and compared to another model without a solder layer. An adjustable user-defined function for the heat release of the RMS during the reaction was used to adopt the reaction front velocity and the combustion temperature to the experimental values. The temperature during the exothermal reaction was recorded at different positions with a time-step size of 10^{-6} s. The measurements suggest that the solder layer can be used to control the peak temperature during the reactive bonding process.

ACKNOWLEDGMENT

This research work was supported by funding from the Deutsche Forschungsgemeinschaft (DFG, German Research Foundation) ¯ Project ID 426204742.

The authors would like to offer many thanks to Andreas Ruh for preparing and performing the cross-sections.

REFERENCES

[1] P. N. Clough and B. A. Thrush, `Mechanism of Chemiluminescent Reaction between Nitric Oxide and Ozone,_ Transactions of the Faraday Society, 1967, vol. 63, pp. 915-925.

[2] T. Geiling, T. Welker, H. Bartsch and J. Mæller, `Design and Fabrication of a Nitrogen Monoxide Measurement Device Based on Low Temperature Co-Fired Ceramics,_ International Journal of Applied Ceramic Technology, 2012, vol. 9, no. 1, pp. 37-44.

[3] T. Welker, T. Geiling, H. Bartsch and J. Mæller, `Design and Fabrication of Transparent and Gas-Tight Optical Windows in Low-Temperature Co-Fired Ceramics,_ International Journal of Applied Ceramic Technology, 2013, vol. 10, no. 3, pp. 405-412.

[4] T. Geiling, T. Welker, C. Ehrling and J. Mæller, `Design, Fabrication, and Operation of a Nitrogen Monoxide Measurement Device Based on LTCC,_ Journal of microelectronics and electronic packaging, 2012, vol. 9, no. 4, pp. 171-177.

[5] K. Malecha and L. J. Golonka, `Microchannel Fabrication Process in LTCC Ceramics,_ Microelectronics Reliability, 2008, vol. 48, no. 6, pp. 866-871.

[6] H. Bartsch de Torres, C. Rensch, M. Fischer, A. Schober and M. Hoffmann, `Thick Film Flow Sensor for Biological Microsystems,_ Sensors and Actuators A: Physical, 2010, vol. 160, no. 1-2, pp. 109-115.

[7] P. Ciosek et al., `Monitoring of Cell Cultures with LTCC Microelectrode Array,_ Analytical and bioanalytical chemistry, 2009, vol. 393, pp. 2029-2038.

[8] J. Wilde, `B4. 1-Trends in Assembly and Packaging of Sensors,_ Proceedings SENSOR 2009, vol. 1, 2009, pp. 205-210.

[9] Y. Fournier, `3D Structuration Techniques of LTCC for Microsystems Applications,_, EPFL, 2010.

[10] P. Uhlig et al., `LTCC Short Range Radar Sensor for Automotive Applications at 24 GHz,_ Proceedings of the IMAPS, 2004.

[11] L. Golonka, P. Bembnowicz, D. JurkÆw, K. Malecha, H. Roguszczak and R. Tadaszak, `Low temperature co-fired ceramics (LTCC) microsystems,_ Optica Applicata, 2001, vol. 41, no. 2, pp. 383-388.

[12] A. Bittner and U. Schmid, `The Porosification of Fired LTCC Substrates by Applying a Wet Chemical Etching Procedure,_ Journal of the European Ceramic Society, 2009, vol. 29, no. 1, pp. 99-104.

[13] T. Thelemann, M. Fischer, A. Groó and J. Mæller, `LTCC-based Fluidic Components for Chemical Applications,_ Journal of microelectronics and electronic packaging, 2007, vol. 4, no. 4, pp. 167-172.

[14] J. Braeuer, J. Besser, M. Wiemer and T. Gessner, `A novel technique for MEMS packaging: Reactive bonding with integrated material systems,_ Sensors and Actuators A: Physical, 2012, vol. 188, pp. 212-219.

[15] H. Jantunen, T. Kangasvieri, J. V±h±kangas and S. Lepp±vuori, `Design aspects of microwave components with LTCC technique,_ Journal of the European Ceramic Society, 2003, vol. 23, no. 14, pp. 2541-2548.

[16] M. Matters-Kammerer et al., `Material properties and RF applications of high k and ferrite LTCC ceramics,_ Microelectronics Reliability, 2006, vol. 46, no. 1, pp. 134-143.

[17] A. Bittner, A. Ababneh, H. Seidel and U. Schmid, `Influence of the crystal orientation on the electrical properties of AlN thin films on LTCC substrates,_ Applied surface science, 2010, vol. 257, no. 3, pp. 1088-1091.

[18] A. S. Rogachev and A. S. Mukasyan, `Combustion of Heterogeneous Nanostructural Systems (Review),_ Combustion, Explosion and Shock Waves, 2010, vol. 46, pp. 243-266.

[19] S. Sen, M. Lake, N. Kroppen, P. Farber, J. Wilden and P. Schaaf, `Self-propagating exothermic reaction analysis in Ti/Al reactive films using experiments and computational fluid dynamics simulation,_ Applied Surface Science, 2017, vol. 396, pp. 1490-1498.

[20] D. P. Adams, `Reactive Multilayers Fabricated by Vapor Deposition (Review),_ Thin Solid Films, 2015, vol. 576, pp. 98-128.

[21] A. J. Gavens, D. Van Heerden, A. B. Mann, M. E. Reiss and T. P. Weihs, `Effect of intermixing on self-propagating exothermic reactions in Al/Ni nanolaminate foils,_ Journal of Applied Physics, 2000, vol. 87, no. 3, pp. 1255-1263.

[22] K. T. Rai Pet al., `CFD analysis of exothermic reactions in Al-Au nano multi-layers foils,_ Materiali in tehnologije, 2011, vol. 45, no. 4, pp. 335-338.

[23] A. Schulz et al., `Characterization of Reactive Multilayer Systems deposited on LTCC featuring different surface morphologies,_ MikroSystemTechnik Congress 2021; Congress. VDE, 2021, pp. 1-5.

[24] A. Schulz, A. Ruh, S. Wiese and J. Mæller, `Characterization of Reactive Multilayer Systems deposited on LTCC screen printing pastes featuring different surface morphologies suitable for reactive joining applications,_ Ceramic Interconnect and Ceramic Microsystems Technologies (CICMT) 2022; Congress, 2022.

[25] E. Wiss, A. Yuile, A. Schulz, J. Mæller and S. Wiese, `Reactive Die Bonding on LTCC Substrates ¯ Analysis by CFD Simulation,_ 24th International Conference on Thermal, Mechanical and Multi-Physics Simulation and Experiments in Microelectronics and Microsystems (EuroSimE). IEEE, 2023, pp. 1-5.

[26] A. Yuile, A. Schulz, E. Wiss, J. Mæller and S. Wiese, `The Simulated Effect of Adding Solder Layers on Reactive Multilayer Films Used for Joining Processes,_ Applied Sciences, 2022, vol. 12, no. 5, p. 2397.

[27] A. Yuile, A. Schulz, J. Mæller and S. Wiese, `Analysis of selective bonding processes using reactive multi-layers for system integration on LTCC based SiPs,_ Microsystem Technologies, 2022, vol. 28, no. 9, pp. 1995-2009.

[28] S. Liang, Y. Zhong, S. Robertson, A. Lio, Z. Zhou and C. Liu, `Investigation of Thermo-mechanical and Phase-change Behavior in the Sn/Cu Interconnects during Self-Propagating Exothermic Reaction Bonding,_ 2020 IEEE 70th Electronic Components and Technology Conference (ECTC). IEEE, 2020, pp. 269-275.

[29] T. Namazu, K. Ohtani, K. Yoshiki, S. Inoue, `Crack propagation direction control for crack-less solder bonding using Ni/Al flash heating technique,_ 2011 16th International Solid-State Sensors, Actuators and Microsystems Conference. IEEE, 2011, pp. 1368-1371.

[30] J. Wang et al., `Joining of stainless-steel specimens with nanostructured Al/Ni foils,_ Journal of applied physics, 2004, vol. 95, no. 1, pp. 248-256.